

# Stress Zones Near Displacement Piers: I. Plastic and Liquefied Behavior

R. L. Handy<sup>1</sup> and David J. White<sup>2</sup>

**Abstract:** Radial stresses measured with the  $K_0$  stepped blade in saturated soils near Rammed Aggregate Piers indicate temporary liquefaction of soil in the vicinity of the rammer. Drainage and compaction proceed during ramming of succeeding layers of the pier, such that the final distribution of radial effective stresses follows plastic cavity expansion theory. A plastic zone and liquefaction can develop only if the radial stress from ramming exceeds the soil compressive strength. If that condition is met, the transient hydrostatic condition allows the zone to expand with additional ramming. A passive condition occurs where radial stresses cannot be fully contained by the overburden pressure, in which case they approximate Rankine passive pressures. The tangential intermediate principal stress then can be modified by ramming of adjacent piers. Stress-induced cracking in the elastic zone contributes to rapid drainage and is discussed in Part II of this two-part series.

**DOI:** 10.1061/(ASCE)1090-0241(2006)132:1(54)

**CE Database subject headings:** Piers; Lateral stress; Soil compaction; Liquefaction; Cavitation; Plasticity.

## Introduction

This is the first of a two-part series reporting and interpreting stresses measured directionally in situ at various depths and distances from Rammed Aggregate Piers. Part I emphasizes changes that occur less than 2 m from centers of the piers, and Part II the changes that occur farther away but nevertheless influence soil behavior closer to the pier.

Piers are rammed in place in layers with a hydraulically driven rammer that is shaped to push the aggregate outward and impose lateral stress on the surrounding soil. Stress measurements were made directionally with the  $K_0$  stepped blade, which uses multiple data points and an extrapolation procedure to remove the effects of soil disturbance from insertion of the blade.

As ideal plastic and elastic behaviors seldom are realized in soils because of volume changes in the plastic zone and nonrecoverable or near-linear responses in the elastic zone, the respective terms will be used without modification in this paper to designate the respective nonideal behaviors. Passive conditions involving uplift are expected at shallow depths where the overburden pressure becomes the minor principal stress.

<sup>1</sup>Distinguished Professor Emeritus, Dept. of Civil, Construction and Environmental Engineering, Iowa State Univ., Ames, IA 50011-3232 (corresponding author). E-mail: rlhandy@iowatelecom.net

<sup>2</sup>Assistant Professor, Dept. of Civil, Construction, and Environmental Engineering, Iowa State Univ., Ames, IA 50011-3232.

Note. Discussion open until June 1, 2006. Separate discussions must be submitted for individual papers. To extend the closing date by one month, a written request must be filed with the ASCE Managing Editor. The manuscript for this paper was submitted for review and possible publication on August 24, 2004; approved on June 9, 2005. This paper is part of the *Journal of Geotechnical and Geoenvironmental Engineering*, Vol. 132, No. 1, January 1, 2006. ©ASCE, ISSN 1090-0241/2006/1-54-62/\$25.00.

## Pier Construction

Rammed Aggregate Piers are constructed by boring vertical holes and backfilling with aggregate that is placed in nominal 0.3 m (1 ft) layers. Each layer is rammed with a beveled rammer as shown in Fig. 1. The rammer is attached to a hydraulic hammer that delivers about 200–300 blows to each layer during about 30 s, after which aggregate for the next layer is dumped and rammed into place. The total energy input per pier is comparable to that from deep dynamic compaction, but is distributed vertically through the depth of the pier instead of being concentrated at the ground surface (Handy et al. 1990). A pier therefore may be considered to represent a vertical confluence of expanding cavities filled with compacted, graded coarse aggregate. Lateral stress imposed on the soil may reduce consolidation settlement by simulating an increase in preconsolidation pressure (Handy 2001).

The rammer is slightly smaller than the hole diameter and is beveled at 45° over one-half of its contact surface to increase lateral displacement and lateral pressures from ramming (Fig. 1). Uplift load tests indicate that side friction is consistent with high contact stress (Caskey 2001; White et al. 2001).

Graded aggregate is used throughout the length of a pier except in the bottom layer that is composed of a coarse, open-graded aggregate. Additional compaction energy is applied on the first lift to create a bulb and form a solid base for compaction of subsequent layers (Fox and Cowell 1998). When required to maintain an open boring, piers are constructed with temporary casing that is incrementally pulled upward prior to ramming each new lift. A schematic diagram showing construction of a pier and some symbols used in this paper is shown in Fig. 2.

## Measuring Lateral In Situ Stress

Lateral stresses were determined with the  $K_0$  stepped blade, which is flat and directional like a Glötzl cell, but is long and incorporates steps having thicknesses of 3.0, 4.5, 6.0, and 7.5 mm. Backpressured pneumatic cells are used to measure soil



**Fig. 1.** Rammer used for layer compaction of Rammed Aggregate Piers

contact pressures on each step, which as shown in Fig. 3, are extrapolated to obtain a hypothetical stress on a zero-thickness blade (Handy et al. 1982, 1990). Tests are rapid and provide a redundancy of data that can be treated statistically.

A linear graph of log pressure versus the step thickness is analogous to a linear void ratio–log pressure relationship, and implies that for a linear relationship to exist, the soil is consolidating laterally in response to pressure from each increase in thickness of the successive steps of the blade. Timed measurements indicate that excess pore pressures are incorporated into the extrapolation, so effective lateral stresses are obtained by subtracting static water pressures (Handy et al. 1982).

### Stepped Blade Data Sets

#### Test Sequence

A boring is made to the first test depth using care to minimize the weight imposed on the drill to avoid changing the soil pressure. Overwashing also must be prevented near the bottom of a boring during wash boring for the same reason. The first blade step is pushed into soil at the bottom of the boring, and the pressure P1

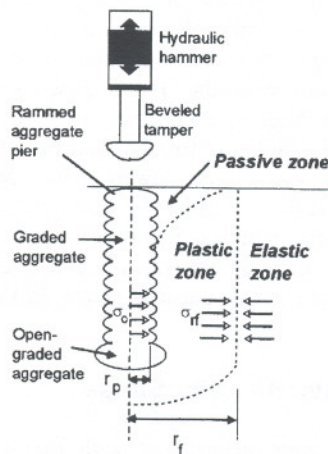


**Fig. 2.** Schematic diagram showing completed pier and anticipated stress zones

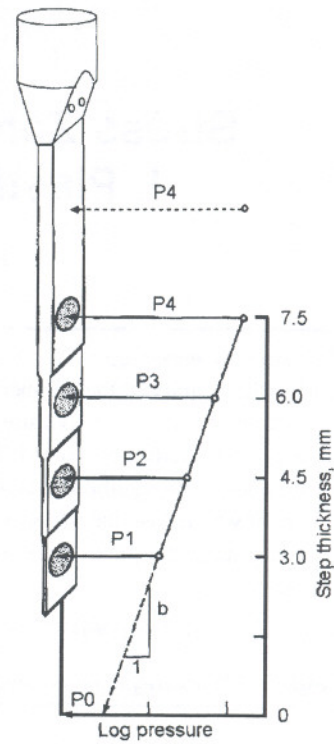


**Fig. 3.** Schematic diagram of  $K_0$  stepped blade showing extrapolation of measured pressures to zero thickness step. Measurements are made during incremental advances so each data set is obtained at constant depth.

in Fig. 3 is measured; then the next step is pushed in and pressure is measured sequentially on P2 and P1 so the time between insertion and reading the cell pressure is approximately the same at each subdepth. Then the next step is pushed and measurements made on cells P3, P2, and P1, and so on until the blade is inserted to its full depth and pressures on all blade cell pressures have been repeatedly measured. An extension of the thickest step allows an additional set of measurements. Each data set consists of four determinations at the shallowest depth, four at the next, three at the next, two at the next, and one (which is a throwaway point) at the fifth and deepest depth. While a total of 14 data points is obtained from each test, the data are not pooled but remain assigned to the respective subdepths. The blade then is pulled and cleaned off, and the boring is advanced to the next test depth where the process is repeated. This results in an incremental, more or less continuous record of lateral stress versus depth. It should be emphasized that the blade is not designed for continuous pushing, which will destroy the instrument. The blade may be used in soft to stiff, fine to coarse-grained soils having a low gravel content.

#### Interpretation

Data points that do not show an increase in pressure with increasing step thickness are automatically excluded from the analysis. This occurs: (1) if the thinnest step does not break down the soil structure, which results in a high first point; and (2) if the thickest step(s) induce a horizontal bearing capacity failure, which results in a reduction in pressure. Such data are not included in the extrapolation to obtain an in situ stress, but may be useful for estimating a modulus and a lateral bearing capacity, respectively. Test records indicate that about one-fourth of the data points typically

are rejected for stress determinations because of one or the other of these reasons, which tend to occur in stiff or soft soils, respectively.

Logarithms of pressures are plotted versus step thickness as shown in Fig. 3, and extrapolated to obtain an estimate of the undisturbed in situ stress,  $P_0$ . A further test for acceptability is the regression coefficient  $R^2$ , which should exceed 0.90 and preferably 0.95. In some instances an acceptable  $R^2$  yields an unlikely value for  $P_0$ . This is most commonly observed in soils containing roots or gravel particles that act as hard spots and increase measured pressures, but also can occur as a result of proximity to empty root channels or animal burrows. Data that appear to be anomalous are retained but labeled with question marks on graphs. Because of the large amount of data obtained, outliers normally do not exert a large influence on central values used for assessments of soil behavior.  $P_0$  data from the several test sites are listed in Table 1 of the Appendix to Part II in this series.

#### Data Plots, Precision, and Accuracy

SBT results from each boring are plotted versus depth. Because tests are not at specific, preselected depths, lines are drawn through maximum and minimum data points in order to define central values and ranges at specific depths. The central value or median and the ranges may be plotted on graphs used for interpretation. Data presented later in this paper indicate that experimental error is about  $\pm 5\%$ , and comparative data have shown excellent agreement with results from self-boring pressuremeter tests (Handy et al. 1982). Agreement generally is poor with interpretations from dilatometer and cone tests that are not intended for this purpose.

### Theoretical Development

#### Plastic Zone (Tangential Minor Principal Stress)

Cavity expansion theory adapted by Baguelin et al. (1978) for interpretation of pressure meter data indicates that radial effective stresses in the plastic zone are distributed according to

$$\sigma_r + c \cot \phi = (\sigma_{rf} + c \cot \phi)(r/r_f)^{K_a - 1} \quad (1)$$

where  $\sigma_r$  = radial stress at a radial distance  $r$  from the center of the expanding vertical cylinder;  $c$  = cohesion;  $\phi$  = friction angle; and  $\sigma_{rf}$  = radial stress at the maximum failure radius  $r_f$  which represents the outer boundary of the plastic zone.  $K_a$  = Rankine coefficient of active earth pressure that is a function of  $\phi$ . If  $c=0$  as a temporary consequence of remolding, Eq. (1) becomes

$$\sigma'_r = \sigma'_{rf}(r/r_f)^{K_a - 1} \quad (2)$$

By taking the logarithm and rearranging the terms, one obtains a linear relationship of the form  $y = a + bx$

$$\log(\sigma'_r) = [\log(\sigma'_{rf}) - (K_a - 1)\log r_f] + (K_a - 1)\log r \quad (3)$$

where the term in the square brackets is constant for a particular soil and depth. A plot of  $\log(\sigma'_r)$  on the  $y$  axis and  $\log r$  on the  $x$  axis therefore should yield a straight line with a negative slope  $b = K_a - 1$ . From the definition of  $K_a$  with  $c=0$ , the slope of the plot is solely dependent on the friction angle—the lower the friction angle, whether from a low value of sliding friction or the development of excess pore pressure, the flatter the negative slope. It should be emphasized that the equation is written for effective stress conditions.

### Liquefaction

The cyclical operation of the hydraulic hammer driving the rammer creates 7–10 Hz compression waves that radiate outward into the surrounding soil. These are followed by shear waves, creating a dynamic condition that is conducive to temporary liquefaction of saturated soil (Mitchell 1982).

Pore-water pressures near piles driven in clay are summarized from the work of many investigators by Poulos and Davis (1979), and may exceed effective overburden pressures close to the piles, indicating a containment of pressure and possible liquefaction. Liquefaction is implied by negative skin friction from reconsolidation of clay near piles after driving (Fellenius and Broms 1969). However, pore-water pressures reported by Chen et al. (1997) indicate that liquefaction did not develop near piles driven in loose hydraulic fill sand. Liquefaction is reported as occurring during installation of stone columns in sand by the vibroflotation method that involves injection of water (Broms 1991). Liquefaction also occurs in susceptible soils as a result of blasting (Charlie et al. 1992). Radial cracking is reported as contributing to rapid drainage of soil temporarily liquefied during deep dynamic compaction (Broms 1991). However, it does not appear that attempts have been made to confirm liquefaction on the basis of lateral stress measurements. Additional evidence supporting liquefaction is presented in Part II of this series.

Liquefaction normally is considered to occur only in granular soils, but analogous thixotropic softening occurs in soft, saturated clays as a result of remolding. Thixotropy involves attractions between ionic double layers and edge-to-face bonding of clay particles, and strength gain is a function of time instead of by drainage alone. However, time-related strength gains also occur in granular soils. No attempt is made to distinguish between the two phenomena in this paper, and a process that produces a liquid through agitation is referred to as liquefaction.

During liquefaction, total stress equals the pore-water pressure, and effective stress is zero. As drainage occurs and pore-water pressure dissipates, total stress will decrease as effective stress increases. This process requires a decrease in total volume, indicating that it probably occurs during compaction of succeeding lifts of a pier. This is discussed in more detail with regard to pore-water pressure measurements presented in Part II.

#### Passive Zone (Vertical Minor Principal Stress)

Wood and Wroth (1977) suggest that passive shearing may occur in soil around an expanding pressuremeter when the minor principal stress is vertical, that is,  $K_0 > 1$ . Passive failure conditions are observed at shallow depths near laterally loaded piles, where the maximum soil resistance is somewhat higher than calculated for the two-dimensional Rankine case (Prakash and Sharma 1989). Mackey (1966) notes that while normal design practice is to assume two-dimensional Rankine conditions near curved surfaces, this is not correct because a convex geometry in effect incorporates a larger volume of soil into the passive zone. However, his analysis also indicates that a high tangential stress inherited from  $K_0$  can reduce the passive coefficient by a substantial amount by tangential arching action. Mackey indicates that the amount of the reduction is proportional to  $K_0$ . If  $\phi = 30^\circ$  and  $K_0$  is at the passive limit, which in this case is 3,  $K_p$  is indicated to be 3.45, close to the Rankine value for the two-dimensional case. The Rankine formula can be modified for a radial geometry by incorporating a dimensionless shape factor,  $S$ , which gives

**Table 1.** Properties of Soils at Test Sites

Site	Memphis	Winterset	Salt Lake City	Des Moines
Soil	Loess	Soil profile in loess	Alluvium	Alluvium
Pedological horizon	C	B and C	C	C
Classification	CL	CH over CL	CL; variable	CL
gwt (m)	2.6	2.0	1.8	1.9
Unit wt (kN/m <sup>3</sup> )	19.6	14.9 and 15.1	17.3	16.5
$\phi'$ from BST	25–26 <sup>oa</sup>	37 and 26°	21°	11–30°
$c'$ from BST (kPa)	0 <sup>a</sup>	8.6 and 8.4	0 <sup>a</sup>	15–38
Liquid limit (%) <sup>b</sup>	33–41	61 and 54	—	—
Plastic limit (%) <sup>b</sup>	18–23	26 and 24	—	—
Moisture (%) <sup>a</sup>	25–26	28 and 25	—	—
Nominal pier diameter (mm)	760	610	910	760
Nominal pier length (m)	4.27	1.22	4.7	5.79

<sup>a</sup>Tested in remolded soil in the passive zone.

<sup>b</sup>From USDA soil profile data and other sources.

$$\sigma'_{rp} = S[\gamma' h \tan^2(45 + \phi'/2) + 2c' \tan(45 + \phi'/2)] \quad (4)$$

where  $\sigma'_{rp}$  = radial effective stress for passive failure;  $S$  = shape factor that for  $\phi = 30^\circ$  can be expected to vary from about 2 to 1.2, the lower amount for overconsolidated soil;  $\gamma'$  = soil unit weight on an effective stress basis;  $h$  = depth below the ground surface; and  $\phi'$  and  $c'$  = angle of internal friction and cohesion on an effective stress basis. If  $c' = 0$ , Eq. (4) simplifies to

$$\sigma'_{rp} = S\gamma' h K_p \quad (5)$$

### Passive/Plastic Boundary

Passive failure of soil adjacent to and near the top of a pier puts a cap on the allowable radial stress in that zone. In unsaturated soil the boundary between the passive and plastic zones can be defined by a simultaneous solution of Eqs. (2) and (5), which gives

$$h = \sigma'_{rr}(r/r_f)^{K_a-1} [K_a/S\gamma'] \quad (6)$$

where  $h$  = depth of passive failure at radial distance  $r$ ;  $\sigma'_{rr}$  = radial stress at the normal plastic failure boundary radius  $r_f$ ; and  $K_a$  = active pressure coefficient. This assumes that cohesion of the soil temporarily is zero from remolding. The shape of the passive zone is that of an inverted cone except that the side slopes are concave upward.

## Lateral Stress Data

### Test Sites

Soil properties at four test sites involving production Rammed Aggregate Piers are shown in Table 1. An advantage of using production piers is that they are not "special." A disadvantage is that after construction is completed, the site is covered by a structure and is unavailable for further tests, so unanswered questions require testing at a different site. Two of the test sites are in fine-grained loessial soils, one in friable, silty loess in Memphis, Tenn., and the other in a plastic loess at Winterset in southern Iowa. The other two sites are in alluvium that is more variable. Lateral stress data for all test sites are listed in Table 1 to the

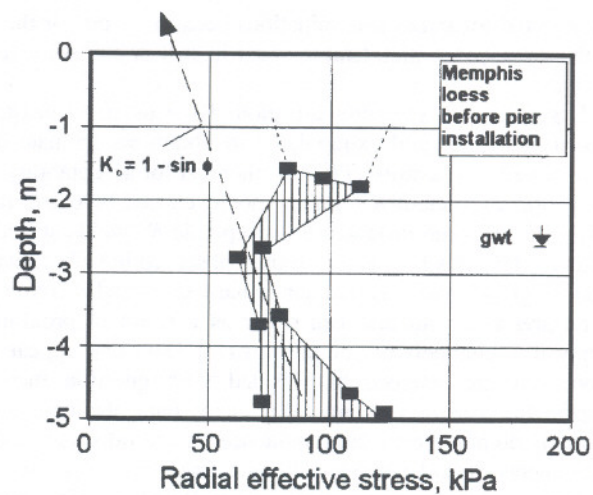


**Fig. 4.** Lateral stresses measured prior to pier installation indicate overconsolidation from removal of overburden and, at shallower depths, from prior construction

Appendix to Part II of this series, where effective stresses were calculated by subtracting the static water pressure from respective total stresses.

### Memphis, Tennessee, Test Site

Soil at the Memphis site is relatively dense CL loess where a building had been removed for construction of a baseball stadium. The soil is overconsolidated as a result of prior construction and removal of unknown amounts of overburden. Overconsolidation is indicated by stress measurements prior to pier installation (Fig. 4), where the increase in lateral effective stress below 2.5 m depth follows a line defined by  $K_0 = 1 - \sin \phi$ , and based on friction angle that was measured by the borehole shear test to vary from 24 to 26°. The average unit weight of the soil estimated from nearby site exploration data to be 19.6 kN/m<sup>3</sup> (125 pcf). As this is a total, not a buoyant, unit weight, the deeper overconsolidation appears to have occurred when the groundwater table was below the lowest depth tested. An estimate of the equivalent overburden can be obtained by extending the trend line to the ordinate as shown by the arrow, and gives 2.6 m (8.5 ft).

High lateral stresses shallower than 2.5 m indicate a higher degree of overconsolidation that probably is relict from the earlier construction.

Production Rammed Aggregate Piers nominally 0.76 m (30 in.) in diameter by 4.3 m (14 ft) long were installed, and radial stresses were measured at five different radial distances. Where data appeared to be inconsistent, tests were repeated in borings made at the same distance along different radial transects from the same pier. The closest previously installed pier was 3 m (10 ft) from the edge of the test pier.

The method of determining median values and ranges of stresses is illustrated in Fig. 5. Ranges were determined graphically by encompassing the measured values in the shaded area, from which a width may be measured at selected depths. Fig. 5 shows stresses measured closest to the pier where outliers are expected as a result of uneven pier expansion during ramming.

The large increase in radial stress at and below the bottom of the pier in Fig. 5 confirms effectiveness of increased ramming to create a bottom bulb. The line representing passive resistance is calculated from the unmodified Rankine coefficient with  $\phi = 25^\circ$

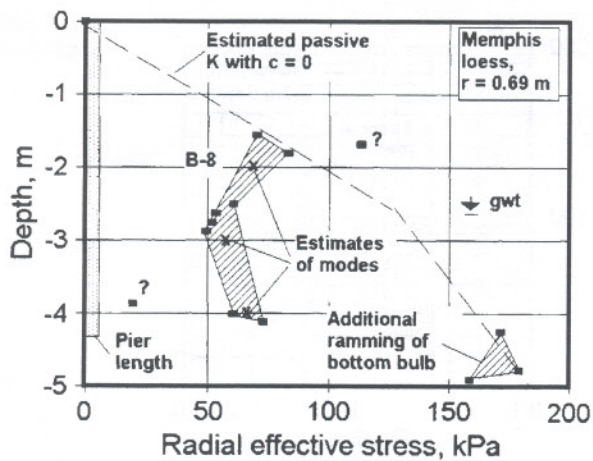


Fig. 5. Radial stresses measured at radial distance of 0.69 m from pier at Memphis test site

and  $c=0$  obtained from borehole shear tests in the remolded soil. It therefore appears that passive conditions can exist even at 4 m depth if rramming is continued long enough. This probably is aided by liquefaction, as will be discussed. Similar graphs were prepared for radial distances of 1.90, 2.21, 3.43, and 4.95 m.

#### Apparent Stress Amplification

It later is shown that the maximum radial stress induced by rramming is of the order of 100–125 kPa, depending in part on resistance of the undisturbed soil. Maximum radial stresses shown in Fig. 5 are 160–175 kPa. Because of the low rramming frequency and short distance from the pier surface to the measurement point, resonant amplification appears unlikely unless it might combine influences of vertical shear waves emanating from the base of the rrammer and compression waves disseminated from the sloping sides. Further research will be necessary to determine possible causes for this discrepancy.

#### Important Inconsistency

On-site plotting of data revealed an inconsistency in radial stress data measured at 1.90 m radial distance, so tests were repeated along a different transect at the same distance from the same pier. Those tests gave the same inconsistency. It later was discovered that all of the measurements fall into one or the other of two populations shown in Fig. 6. A statistical *t-test* shows less than a 0.3% probability that the data represent a single population. The radial distance of 1.9 m therefore appears to define a boundary between two discrete soil behaviors. The decrease in stress within this zone is consistent with stress relief from rramming, which suggests that this is the anticipated boundary between plastic and elastic behavior. Boring B-5 may have received an additional nudge because it was closer to an adjacent pier than B-4, but the stepped blade was oriented to try and minimize that influence. Both data populations reflect the increased radial stress from extra rramming on aggregate in the bottom of the pier.

Lateral stresses prior to pier installation (Fig. 4) all exceeded 60 kPa, whereas stresses in the lower population of Fig. 6 are less than 50 kPa, indicating that pre-existing lateral stress is relieved in the plastic zone. On the other hand, most of the stresses in the higher population in Fig. 6 are higher than the measured pre-existing field stresses, indicating that outside of the plastic zone rramming stress must be additive to the field stress. The total radial stress in the elastic zone exceeds the passive limit calculated with

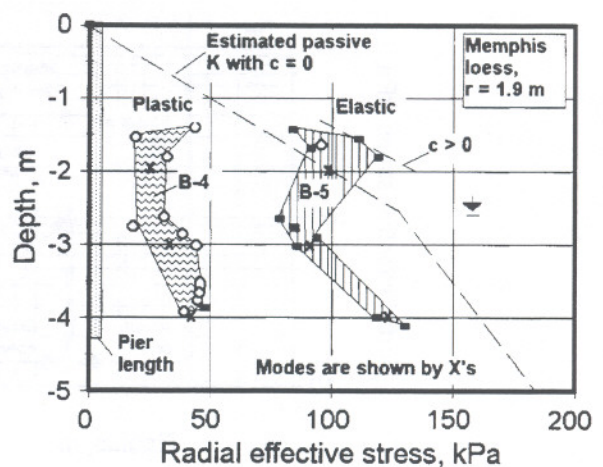


Fig. 6. Two data populations at same radial distance appear to define boundary between plastic and elastic behavior

$c=0$ , a further indication that soil in the elastic zone has not been remolded. The maximum radial stress in Fig. 6 is about 125 kPa, which is consistent with the maximum stress deduced to occur at the pier surface during rramming.

The retention of high radial stress outside of a zone of stress relief appears to violate static equilibrium unless there is arching action in the elastic zone. This matter is treated in Part II of this series.

#### Comparison of Data with Theoretical Stress Distributions

The form of Eq. (3) indicates a linear relationship between radial stress and distance when plotted on logarithmic axes. (As will be shown in Part II, this also is the case for a modified elastic distribution, so similar graphs are used in that presentation.) Median radial stresses and stress ranges measured at depths of 2, 3, and 4 m at the Memphis site are plotted in a logarithmic format in Fig. 7. The apparent plastic/elastic boundary at 1.9 m is shown on all three graphs in this figure, which therefore defines the plastic zone as cylindrical and vertically oriented with a constant radius. This suggests that the contribution of variations of the intermediate principal stress with depth is relatively small or nonexistent.

Unfortunately, data were not obtained at radial distances between 0.69 and 1.9 m, so it is not possible to confirm the predicted logarithmic linearity of stresses in the plastic zone at this site. However, linearity was confirmed by tests at the Salt Lake City, Utah site, as shown later in this paper.

#### Pier Contact Pressure

Lines extended through the median data at 0.69 and 1.9 m radii in Fig. 7 give highly variable values for  $K_a$ , but averaging the data gives  $K_a=0.33$  and  $\phi=30^\circ$ , which is higher than the value of  $25^\circ$  measured prior to pier installation. Lines drawn in accordance with the average  $K_a$  are shown by dashed arrows in Fig. 7, and for the most part are incorporated into the observed data ranges, the exception being in the transition zone at 1.9 and 4 m depth. Extending the arrows to the nominal pier radius gives pier contact pressures of about 100 kPa (1 Tsf). Pier expansion during rramming is not accounted for in the extrapolation. A similar extrapolation of data from a Rrammed Aggregate Piers test site in sandy alluvial soil in Salt Lake City, Utah gave 115 and 120 kPa. As contact pressure develops in response to resistance of the soil to pier expansion, it may be expected to be lower in soft than in stiff soils.

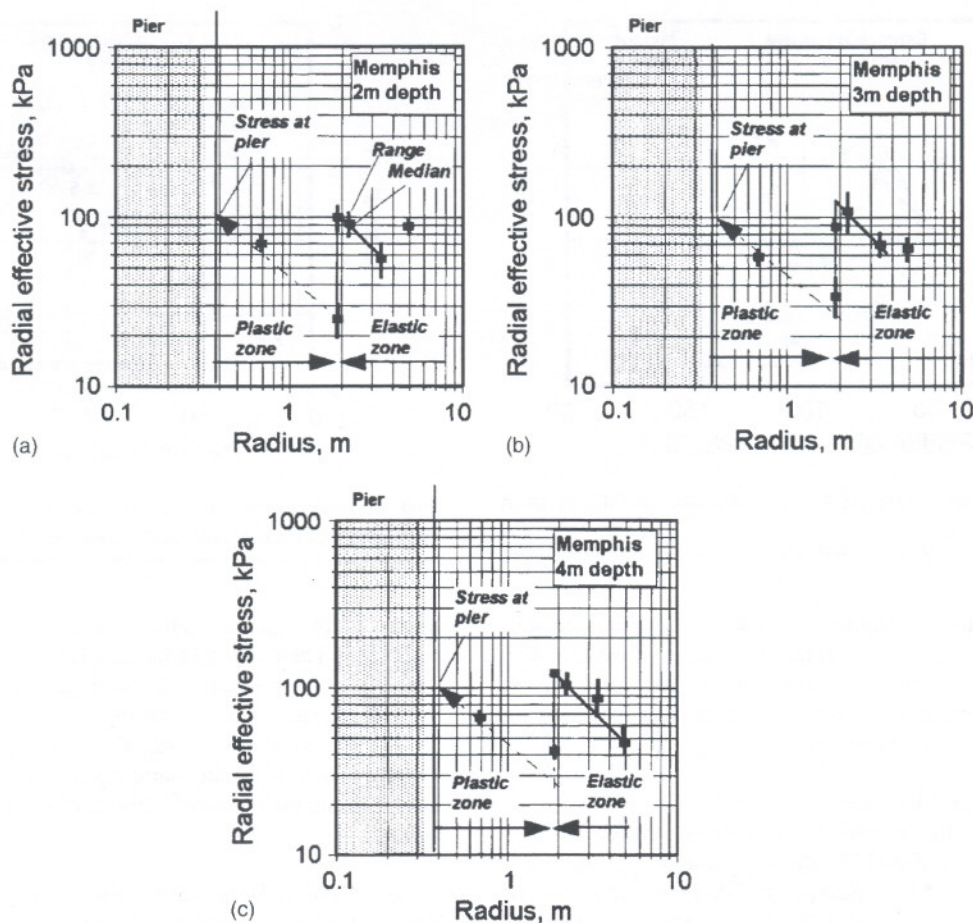


Fig. 7. (a), (b), and (c) Logarithmic plots showing the mode and range of radial stress determinations versus radial distance at Memphis site. The plastic zone is discussed in this paper, and the elastic zone is discussed in Part II.

#### Compaction of Plastic Zone

Backcalculated friction angles are very sensitive to the slope of the stress-distance line, so a more reliable indication of compaction is the inference that water is ejected from the plastic zone during ramming. Evidence for this is presented in Part II of this series.

#### Liquefaction and Radius of Liquefied Zone

The sawtooth graphs in Fig. 7 indicate that radial stress at the outer boundary of the plastic zone is very nearly equal to radial stress developed at the pier surface during ramming. This transfer of stress is quite extraordinary, and is possible if the intervening soil temporarily is liquefied during ramming. This also would mean that soil at the outer boundary of the liquefied zone provides the reaction necessary to create a contact pressure at the surface of the pier.

As liquefaction occurs, pressure is transferred as total stress that is hydrostatically distributed and should remain nearly constant throughout the liquefied zone regardless of distance or direction. It therefore can be expected that the liquefied zone will continue to enlarge as long as ramming continues, which is supported by the data in Fig. 5 as well as by materials balance observations made during pier construction. The radial compressive strength of soil at that boundary must be exceeded to permit remolding and hence liquefaction, which means that if radial stress does not equal or exceed the horizontal compressive strength of the soil, there can be no remolding, no liquefaction, and no plastic zone.

#### Stress Sequence in Liquefied Zone

The above analysis suggests the following sequence may occur during ramming of each pier segment in saturated soil:

1. Repetitious ramming energy causes temporary liquefaction of a bulb of saturated soil adjacent to the pier and below the level of the rammer head. As ramming continues, the bulb enlarges, but there should be little likelihood of a breakout of liquefied soil so long as it is confined by the previously rammed lift and by competent soil. However, localized weakness may allow liquefied material to be ejected outward and/or upward, as will be indicated later in this paper. Liquefied soil also injects into radial cracks developed at the boundary with the elastic zone, which is discussed in detail in Part II.
2. Outward drainage of excess water from the liquefied soil allows a transition from total to effective stress. The loss of water and corresponding decrease in volume are driven in part by compaction of the next aggregate layer. The final distribution of radial effective stresses in the plastic zone appears to follow plastic state cavity expansion theory, that is, with the major principal stress radial and the minor stress tangential. This may be subject to change from ramming of adjacent piers.

#### Radius of Plastic Zone without Liquefaction

Only limited testing was conducted above a groundwater table, but on the basis of the above interpretations some predictions can be made. Without the stress transfer mechanism from liquefac-

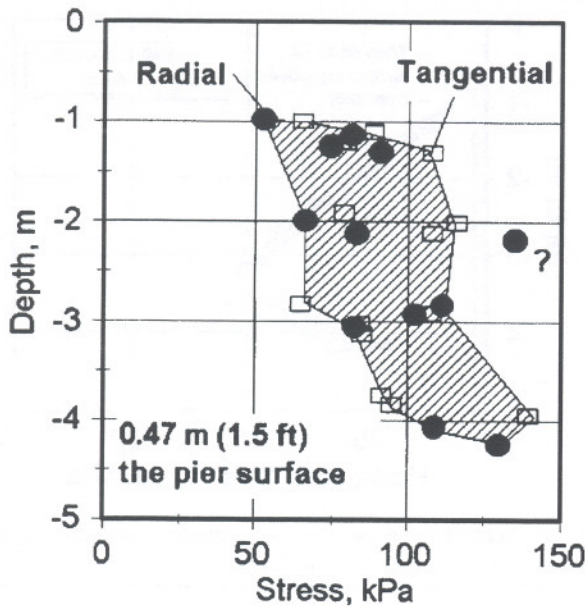


Fig. 8. Radial and tangential stresses measured near pier in alluvial soil at Des Moines test site

tion, radial stress will be transmitted according to cavity expansion theory that as indicated in Eq. (2) is governed by  $K_0$  and the friction angle of the soil. Calculations indicate that this typically should cause about a 50% reduction in radius of the plastic zone, but this will vary depending on the strength of the soil. A high tangential stress inherited from  $K_0$  will tend to further restrict the development of a plastic zone.

#### Calculation of Passive Zone

Although tests were too shallow at the Memphis site to detect a passive zone, it can be calculated from Eq. (6). Data in Fig. 7(a) indicate that at 2 m depth  $\sigma_{rt} = 22$  kPa at  $r_f = 1.9$  m. Substituting values for the soil unit weight and friction angle ( $\gamma' = 19.6$  kN/m<sup>3</sup>,  $\phi = 25^\circ$ ) and using a conservative  $S = 1$ , at the pier boundary the depth of passive failure is  $h = 1.2$  m. A similar calculation for depth of the plastic zone at the outer limit of the plastic zone gives  $h = 0.46$  m. However, these are maximum depths that are based on the soil having no cohesion.

#### Des Moines Test Site

##### Radial and Tangential Stress

Radial and tangential stresses respectively are major and minor principal stresses in the plastic zone, but that may be subject to change from ramming of an adjacent pier. Stress measurements therefore were made at a radial distance of 0.85 m from the center of a 0.76 m diameter (30 in.), 5.79 m (19 ft) long pier in a line of piers spaced 1.8 m center-to-center. The test pier is part of an array of production piers used to reduce settlement of a road embankment at Des Moines, Iowa (White et al. 2001). Soil information is included in Table 1 and stress data are in the Appendix to Part II.

As shown in Fig. 8, radial and tangential stresses are virtually equal, suggesting a possible reliquefaction that can occur if there is a further increase in density of saturated soil in the plastic zone of a finished pier. Both stresses increase with depth. Overlapping stress zones are illustrated in Fig. 9.

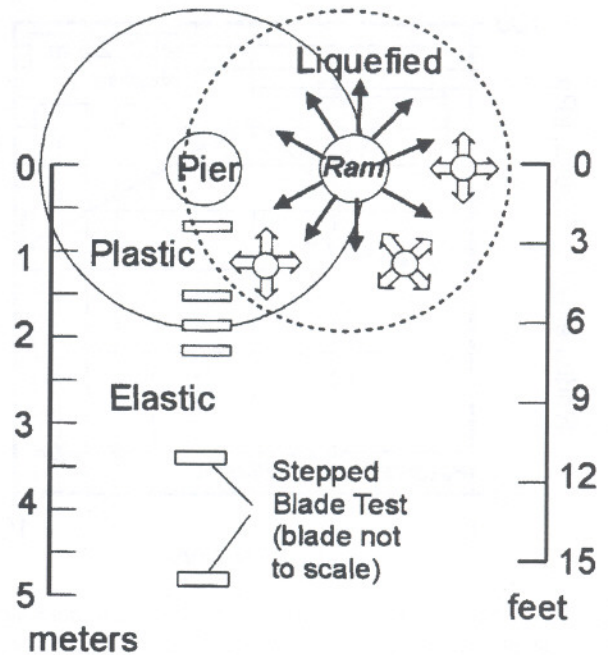


Fig. 9. Influence of ramming of adjacent pier on tangential intermediate principal stress

#### Winterset Test Site

Although the first measurements of lateral in situ stress near rammed aggregate piers were made at the Winterset site, it was not until tests were performed and analyzed at other sites that the significance of the early tests was more fully realized.

Soil at the Winterset site is plastic, clayey loess with the upper 1 m weathered to stiff, expansive clay. This layer is referred to by soil scientists as a "B horizon," and has a characteristic blocky structure as a result of seasonal volume changes related to moisture content. Overlying the B horizon was a topsoil layer called the "A horizon" that was removed prior to construction.

Radial stresses measured at radial distances of 1.0, 1.3, and 3.1 m are shown in Fig. 10. Stresses induced by ramming of a bottom bulb are highest closest to the pier and decrease outward, as also observed at the Memphis site. Particularly significant is that the influence of ramming extends to a depth that is over a pier length below the bottom of the pier. This can be attributed to the

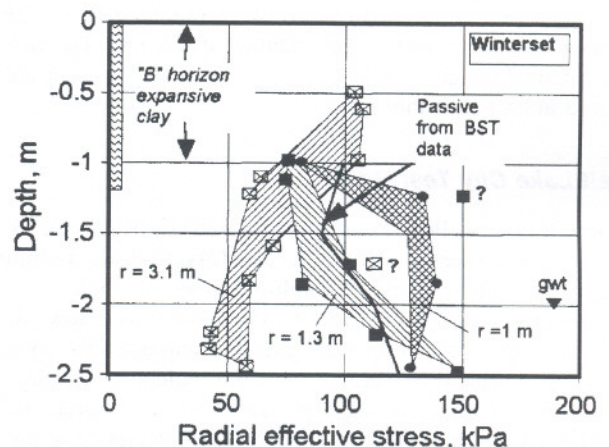


Fig. 10. Radial stresses measured at Winterset site

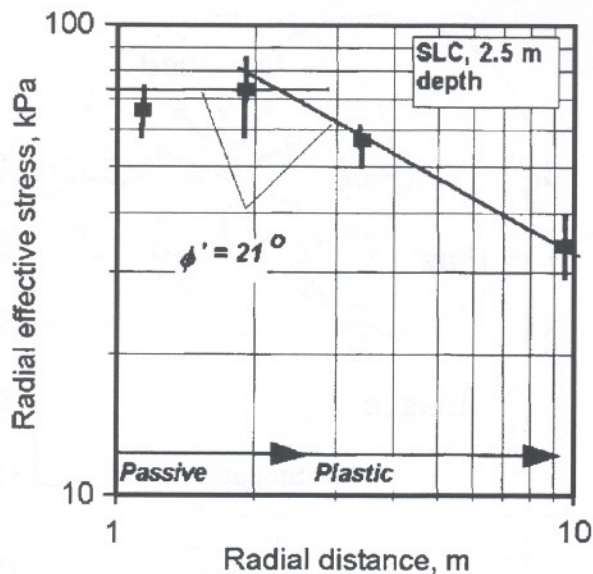


Fig. 11. Radial stresses measured in zone of soft soil near rammed aggregate pier installed alluvium at Salt Lake City test site, with passive and plastic stress lines calculated using  $\phi' = 21^\circ$  from borehole shear tests

very soft nature of the saturated loess below the B horizon and possible temporary liquefaction in this zone. The extension of stress into the soft zone is of obvious practical importance for extending the effective depth of the soil reinforcement below the bottom of a pier. Radial stresses measured close to and below the bottom of the pier exceed passive limits obtained from the friction angle measured in the undisturbed soil. As these stresses were measured in remolded soil with a cohesion of zero, they suggest compaction of soil adjacent to the pier.

The pre-existing field  $K_0$  lateral stress was determined to be high in the B horizon, attributed to seasonal shrinkage cracking and crack filling of the expansive clay. Boring and placement of the pier resulted in about a 30% reduction in radial stress, and the indicated 75 kPa is less than that which would have been transferred from ramming had the soil been liquefied. This is explained if the compressive strength in the B horizon prevented remolding and liquefaction. The passive resistance at 1 m depth calculated from data in Table 1 is 77 kPa times a shape factor, Eq. (4).

Radial cracks about 2 m long were observed at the ground surface emanating from piers installed at this site. The field observation of radial cracking confirms interpretations that are presented in Part II of this series.

### Salt Lake City Test Site

A soft, saturated silt layer was encountered at a depth of 2–3 m in alluvium at a research site in Salt Lake City, Utah where Rammed Aggregate Piers were used for uplift anchors. Borehole shear tests gave  $\phi' = 21^\circ$  compared with  $30\text{--}39^\circ$  above and below the soft layer. The piers therefore were extended through this layer, and  $K_0$  stepped blade tests were performed. An older model blade was used that had an inoperative pressure cell, so in order to gain precision the slopes of the stepped blade thickness–log pressure diagrams were averaged (Handy et al. 1982).

Results in Fig. 11 show a linear logarithmic relationship pre-

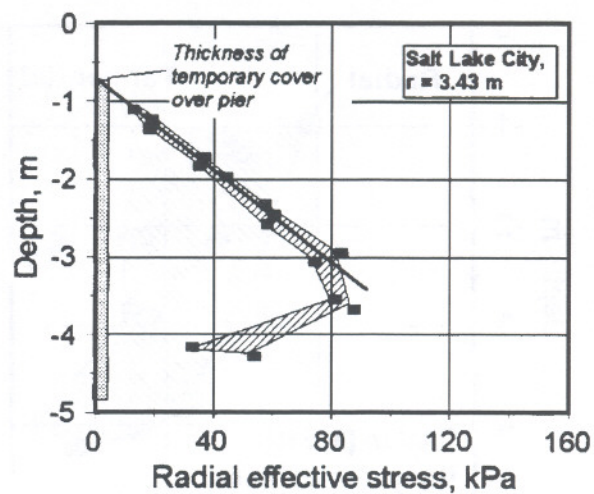


Fig. 12. Stepped blade data indicating passive conditions in what is believed to be displaced soft silt layer

dicted by cavity expansion theory for the plastic zone. The slope of the line in the plastic zone is drawn for  $\phi = 21^\circ$  obtained from borehole shear test (BST) data.

Closer to the pier, radial stress is relatively constant, suggesting a passive condition, probably a result of localized liquefaction of the soft layer during ramming. The horizontal stress line was drawn on the basis of uncorrected  $K_p$  based on the measured  $\phi = 21^\circ$ , and an average overburden unit weight of  $17.3 \text{ kN/m}^3$  (110 pcf). A decrease in stress close to the pier also was found at other depths and may relate to the development of moderate arching action in the plastic zone as excess pore pressure in soil adjacent to the pier dissipated into the pier.

Stresses measured at a radial distance of 3.43 m show an unusual linear relationship to depth (Fig. 12). Extension of the trend line to intersect the ordinate gives an estimate of 0.6 m for the thickness of soil placed on top of the pier. A minimum thickness of 0.3 m was specified to protect the pier from construction traffic. A similar extrapolation of lateral stress versus distance data can provide a clue to how much overburden has been removed (Handy et al. 1990).

A linear relationship to depth suggests a possible passive condition that can allow backcalculation of a friction angle. Because the soil cover was added after the pier was completed, it is appropriate to use the net depth in that calculation. The level of the groundwater table was not measured at this boring location. Without the influence of static pore water pressure the data are linear to a larger depth. In either case the backcalculated  $\phi' = 19.3^\circ$  based on an average unit weight of the overburden of  $17.3 \text{ kN/m}^3$  (110 pcf). If the overburden unit weight is that of the displaced soil, estimated to be  $15.7 \text{ kN/m}^3$  (100 pcf), the backcalculated friction angle is  $22^\circ$ , in closer agreement with that measured with the BST.

A linear increase of stress with depth did not appear in borings closer to or farther from the pier. Because soil showing this relationship cuts through shallower layers having a significantly higher friction angle, soil from the soft layer may have become liquefied during ramming, then pushed outward and upward into a zone of lower confining stress. Such displacement should be beneficial to performance of a pier. The uplift piers were subjected to a vigorous regime of repeated loading and showed only moderate deflection (Lawton and Merry 2000).

As shown at the right in Fig. 11, radial stress measurements in

the soft layer suggests that the plastic boundary extends farther than 10 m, which is the limit of the measurements. This compares with 4–5 m at other depths, and is consistent with the premise that the position of the plastic/elastic boundary depends in part on firmness of the resisting strata.

The data in Fig. 12 are an indication of the precision attainable with the  $K_0$  stepped blade, which in this case is on the order of +5%.

## Conclusions

Measurements of radial and tangential stresses near Rammed Aggregate Piers with the  $K_0$  stepped blade indicate that transient liquefaction can occur in saturated soil near the rammer if the lateral stress exerted by ramming exceeds the compressive strength of the soil. Liquefaction allows ramming stress to be transmitted outward with little or no reduction in pressure, such that the plastic zone may continue to enlarge as long as ramming and liquefaction continue. Part II presents evidence that excess pore water drains outward into the elastic zone, which allows the temporarily liquefied soil to be compacted during ramming of subsequent lifts.

## Acknowledgments

The writers gratefully acknowledge the suggestions and contributions of Dr. Kord Wissman to this investigation. The Winterset and Memphis tests were conducted by GeoSystems Engineering, Inc., Lenexa, Kan., under a research contract sponsored by the U.S. Army Corps of Engineers Waterways Experiment Station, Dr. Glen Ferguson, Principle Investigator. The Salt Lake City tests were sponsored by Geopier Foundation Company Northwest, Inc., Portland, Ore., Geopier Foundation Co., Inc., Scottsdale, Ariz., the Federal Highway Administration, and the University of Utah, Dr. Evert Lawton the Principal Investigator. Des Moines tests were conducted as part of a research project of the Spangler Geotechnical Laboratory at Iowa State University sponsored by the Iowa DOT. The writers acknowledge the contributions of Dr. Scott Mackiewicz in conduct of some of the tests and for suggesting an important design modification for the  $K_0$  stepped blade. In particular the writers acknowledge the foresight and support of engineers of the US-DOT-FHWA, who in the late 1970s saw the need for and initiated a program to develop an instrument to accurately measure lateral in situ stress directionally in soils. This eventually led to invention and development of the  $K_0$  stepped blade. The writers also acknowledge the support and participation of many other colleagues and co-workers who

helped to make it happen, and in particular Dr. Nathaniel Fox, who initiated the stepped blade research and later founded Geopier Foundation Co., Inc. The writers serve as research consultants for Geopier, a subsidiary of the Tensar Corporation.

## References

- Baguelin, F., Jézéquel, J. F., and Shields, D. H. (1978). *The pressuremeter and foundation engineering*, Trans Tech Publications, Clusathal, Germany.
- Broms, B. (1991). "Deep compaction of granular soils." *Foundation engineering handbook*, 2nd Ed., H. Y. Fang, ed., 814–832.
- Caskey, J. M. (2001). "Uplift capacity of rammed aggregate pier soil reinforcing elements." MS thesis, Univ. of Memphis, Memphis, Tenn.
- Charlie, W. A., Jacobs, P. J., and Doehring, D. O. (1992). "Blast-induced liquefaction of an alluvial sand deposit." *Geotech. Test. J.*, 115(1), 14–23.
- Chen, C.-H., Yang, W.-H., and Sutu, Y. W. (1997). "Ground responses during pile driving." *Proc., 14th Int. Conf. SMFE*, Vol. 1, 457–460.
- Fellenius, B. H., and Broms, B. B. (1969). "Negative skin friction for long piles driven in clay." *Proc., 7th Int. Conf. SMFE*, Vol. 2, 93–98.
- Fox, N. S., and Cowell, M. (1998). *Geopier foundation and soil reinforcement manual*, Geopier Foundation Company, Scottsdale, Ariz.
- Handy, R. L. (2001). "Does lateral stress really influence settlement?" *J. Geotech. Geoenviron. Eng.*, 127(7), 623–626.
- Handy, R. L., Mings, C., Retz, D., and Eichner, D. (1990). "Field experience with the back-pressured  $K_0$  stepped blade." *Transportation Research Record*, 1278, Transportation Research Board, Washington, D.C., 125–134.
- Handy, R. L., Remmes, B., Moldt, S., Lutenecker, A. J., and Trott, G. (1982). "In situ stress determinations by Iowa stepped blade." *J. Geotech. Eng. Div., Am. Soc. Civ. Eng.*, 108(11), 1405–1422.
- Lawton, E. C., and Merry, S. M. (2000). "Performance of Geopier-supported foundations during simulated seismic tests on northbound Interstate 15 Bridge over South Temple, Salt Lake City, Utah." *Rep. No. UUCVEEN 00-03*, Dept. of Civil and Environmental Engineering, Univ. of Utah, Salt Lake City, Utah.
- Mackey, R. D. (1966). "Active and passive pressures on curved surfaces." *Sols Soils*, 17, 31–40.
- Mitchell, J. K. (1982). "Soil improvement—State of the art report." *Proc., 10th Int. Conf. on Soil Mechanics and Foundation Engineering*, Vol. 4, A. A. Balkema, Rotterdam, The Netherlands, 509–566.
- Poulos, H. G., and Davis, E. H. (1979). *Pile foundation analysis and design*, Wiley, New York.
- Prakash, S., and Sharma, H. D. (1989). *Pile foundations in engineering practice*, Wiley, New York.
- White, D. J., Lawton, E. C., and Pitt, J. M. (2001). "Lateral earth pressure induced from rammed aggregate piers." *Proc., 53rd Canadian Geotechnical Conf.*, Vol. 2, Montreal, 871–876.
- Wood, D. M., and Wroth, C. P. (1977). "Some laboratory experiments related to the results of pressuremeter tests." *Geotechnique*, 27(2), 181–201.